Dynamic Torque and Drag Model

Conference Paper · October 2020

DOI: 10.2118/201629-MS

2 authors:

Robello Samuel
University of Southern California
253 PUBLICATIONS **1,647** CITATIONS
SEE PROFILE

Wenjun Huang
China University of Petroleum Beijing
31 PUBLICATIONS **404** CITATIONS
SEE PROFILE

Please fill in the name of the event you are preparing this manuscript for.	SPE Annual Technical Conference and Exhibition to be held 5 – 7 October 2020 in Denver, Colorado, USA.
Please fill in your 6-digit SPE manuscript number.	SPE-201629-MS
Please fill in your manuscript title.	Dynamic Torque And Drag Model

Please fill in your author name(s) and company affiliation.

Given Name	Surname	Company
Robello	Samuel	Halliburton
Wenjun	Huang	Halliburton

Abstract

It is generally acceptable to use soft string model for simple wells and stiff string for high dogleg wells. But these models fail to reveal the complex mechanical behaviors of tubular string in tripping in, tripping out, and sliding drilling operations with time as some segments of tubular string may move upward and downward alternatively. As a result, the model under predicts or over predicts the behaviors of tubular string, and requires multiple calibrations of friction factor. To avoid this, a new model has been developed to estimate dynamic torque and drag. In the new model, the effects of tubular displacement, drill fluid, viscous force, and velocity-dependent friction force are all considered, which overcomes the shortcomings of all previous models. The new model can be used for calculating dynamic mechanical behaviors of tubular string under tripping in, tripping out, and sliding drilling operations. The results provide new insights that have not been previously presented and will provide valuable insights into well planning and designing.

Introduction

The most conventional torque and drag model is the soft string model by Johancsik et al. (1984). In the soft string model, the tubular string is simplified as a soft rope with zero bending stiffness. Soft string model have been successfully used in drilling practice. To overcome the shortcomings of soft string model, Ho (1988) presented the stiff string model in which the tubular string is assumed to be a thin elastic rod. Compared with soft string model, the bending stiffness of tubular string is further considered. Gao (1994) derived the integral mechanical model of tubular strings from the basic equations of down-hole tubular strings. Wu (1995) studied the axial force transfer in horizontal wellbore and gave the expression of slack off limit. McSpadden (2002) presented the tubular string model in which the tubular string body between connectors is taken as beam-column and connectors contact with wellbore. Mitchel and Samuel (2009) brought out the limitations of soft string models under certain conditions including the real weakness of the torque-drag model in the use of constant curvature wellbore trajectories. They also presented a new model with bending stiffness. Mitchell (2015) assumed that connectors and mid-points of tubular string bodies are the potential contact points and built the integral model of tubular strings. Yuan and Samuel (2019) introduced the alternating soft and string model depending on the wellbore profile and stiffness of

the pipe so that calculations can be faster so as to be adopted for real-time operations. Several other researchers presented various models, but the fundamental concepts remained the same.

In the above models, static equilibrium of tubular string is adopted and dynamic loads in tubular string movement are neglected. This simplification in derivation is usually reasonable for most states of tubular string movement, but will lead to unneglectable deviations under some cases. For example, in the starting stage of tripping out operation, tripping out velocity increases with time and thus the hook load is usually larger than that under stable state. However, the static models cannot reveal the amplification of hook load in tripping out operation.

In 2015, Miska et al. proposed an improved dynamic soft string model in which the effects of velocity and acceleration are taken into consideration. An important assumption is made in Miska's (2015) model but not explicitly explained in his paper. The assumption is that elastic axial vibration is neglected and the axial velocity along the entire tubular string is constant at every moment. To be specific, the values of velocities along the entire tubular string are all equal to tripping velocity on the hook. Therefore, the axial movements of the entire tubular string are completely synchronous. Considering that the surface displacement, velocity, and acceleration are given in advance, the mechanical model can be easily solved similar to the conventional soft string model.

However, complex mechanical behaviors of tubular string may not be revealed with the introduction of the above assumption. To overcome this shortcoming, the above assumption is taken out in the new model and tubular displacement is further considered. Friction factor is taken as a constant value related to tripping direction in previous models. However, this simplification of friction factor is not always reasonable. Even in the tripping out operation, some segment of the tubular string may move upward and downward alternatively, and the friction force should be tubular velocity dependent. Meanwhile, drill fluid also has a major effect on tubular mechanical behaviors. Therefore, in the new model, the effects of tubular displacement, drill fluid, and velocity-dependent friction force are all considered. With the new model, the complex mechanical behaviors of tubular string in tripping in, tripping out, and drilling operations are revealed.

Results show that neglecting tubular elasticity leads to underestimation or overestimation of hook load in tripping operations, which further leads to risky design results. The nonlinearity of friction force in tubular displacement cannot be neglected. It has been found that friction force can substantially inhibit tubular movement, and the nonlinearity of friction force plays an important role in in tubular displacement. For example, the magnitude of displacement decreases quickly and then vanishes after tripping in and out operations due to friction force. To ensure a larger tripping safety factor, a gentler hook control mode should be adopted. Also, the stable hook loads after tripping in and out operations are usually different from the initial values. Applying external vibrating force on tubular string can decrease the drag. For example, oscillating weight on bit (WOB) can increase hook load compared with the constant WOB estimation. The effect of drag reduction due to vibrating force increases with the increase in displacement magnitude. Explicit central finite difference scheme of the tubular displacement equation and Karnopp's friction model are adopted in the calculation. Results indicate that the calculation algorithm is fast and stable.

Theoretical Model

Assumptions

The following assumptions are adopted in the tubular displacement model:

(1) Tubular string is assumed to be a soft rope with zero bending stiffness.
(2) Tubular string is in continuous contact with the wellbore and the deflection of tubular string is in consistent with the wellbore axis.
(3) Only axial displacement is taken into consideration, whereas lateral and torsional displacement are neglected.

(4) Value of friction factor is related to velocity. To be specific, friction factor is determined by velocity direction when velocity is not zero and determined with tubular equilibrium equation when velocity is zero.
(5) The inner and annular fluid flows are always stable. In other words, pressure displacement of fluid flow is neglected.

Note that assumptions (1) and (2) are also adopted in conventional soft string model. Unlike the conventional soft string model, axial displacement, velocity-dependent friction force, and fluid effect are further considered with assumptions (3)-(5).

Tubular Movement Model

Taking a segment of tubular string shown in Eq. 1 as research object, the dynamic equation of tubular string in fluid environment can be deduced on the basis of Newton's second law.

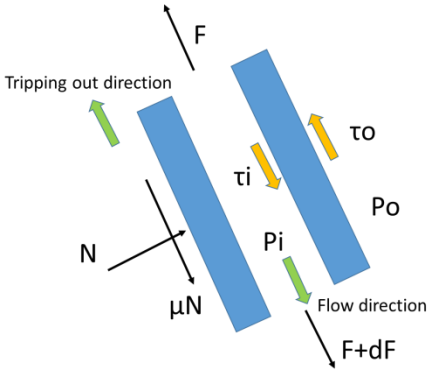

Figure 1 A segment of tubular string

$$\frac{\partial F}{\partial s} + q_e \cos\varphi + \mu N + \pi\tau_{wi}D_i - \pi\tau_{wo}D_o = \rho_s A_s \frac{\partial v}{\partial t} \quad (1)$$

where F is the equivalent axial force on tubular string and is calculated by

$$F = F_a - P_i A_i + P_o A_o \quad (2)$$

where F_a is the actual axial force on tubular string, P_i and P_o are the inner and annular pressures, D_i and D_o are the inner and outer diameters of tubular string, A_i and A_o are the areas calculated from inner and outer diameters of tubular string.

In Eq. 1, q_e is the equivalent tubular string weight per unit length and is calculated by

$$q_e = \rho_s A_s + \rho_i A_i - \rho_o A_o \quad (3)$$

where ρ_s, ρ_i, and ρ_o are the densities of tubular string, inner fluid, and annular fluid, and A_s is the area of cross-section of tubular string.

In Eq. 1, φ is the inclination angle of well trajectory, μ is the friction factor between tubular string and wellbore surface, N is the contact force between tubular string and wellbore per unit length and is calculated by

$$N = \sqrt{\left(Fk + q_e n_z - \rho_s A_s \left(\frac{dv}{dt}\right)^2\right)^2 + (q_e b_z)^2} \quad (4)$$

in which, k is the curvature of well trajectory, n_z and b_z are the normal and bi-normal Frenet-Serret unit vector components in the vertical direction, v is the axial velocity of tubular string.

The axial strain of tubular string under the effects of axial force and pressures is calculated by

$$\frac{\partial u}{\partial s} = \frac{1}{EA_s}\left(F + (1-2v)(P_iA_i - P_oA_o)\right) \quad 5$$

where v is the Poisson ratio of tubular string.

Substituting Eq. 5 into Eq. 1, we obtain the displacement equation of tubular string,

$$\rho_s A_s \frac{\partial^2 u}{\partial t^2} = \frac{\partial}{\partial s}\left(EA_s \frac{\partial u}{\partial s}\right) + q_e cos\varphi + \mu N + \pi\tau_{wi}D_i - \pi\tau_{wo}D_o \quad 6$$

Friction model

Simulation of friction force is difficult because of its strong nonlinear behavior when velocity direction changes. More details on the friction factors for various operations are discussed by Samuel.R (2010). In this study, Karnopp (1985)'s friction model is adopted in the string movement model.

A small region of velocity near zero is defined as $|v| < \delta$ shown in Figure 2. Outside this region, friction factor is expressed as the function of velocity, which corresponds to sliding friction state. Inside the region, the friction force F_f should be calculated first with equilibrium equation. If the friction force is larger than the maximum sticking friction F_s, the friction factor is determined by velocity and friction is in the sliding state. If the friction force is smaller than the maximum sticking friction force, the friction factor is calculated from equilibrium equation and friction is in the sticking state. Therefore, the value of friction factor can be obtained from Eq. 7.

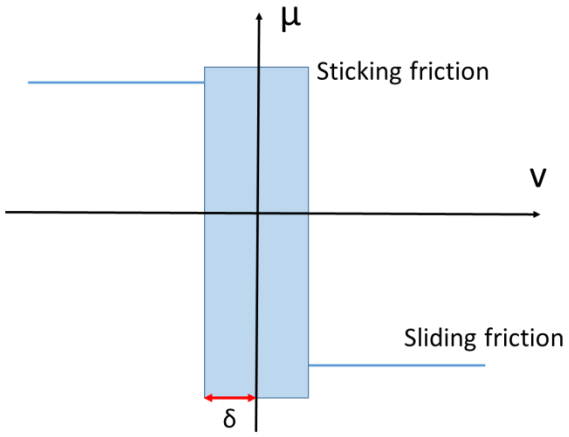

Figure 2 Schematic of friction model

$$\mu = \begin{cases} calculating\ from\ equilibrim\ equation & if\ |v| < \delta\ and\ F_f \le F_s = \mu_s N \\ -sign(v)\mu_d & else \end{cases} \quad 7$$

in which, μ_d is the sliding friction factor and μ_s is the maximum sticking friction factor.

Fluid flow model

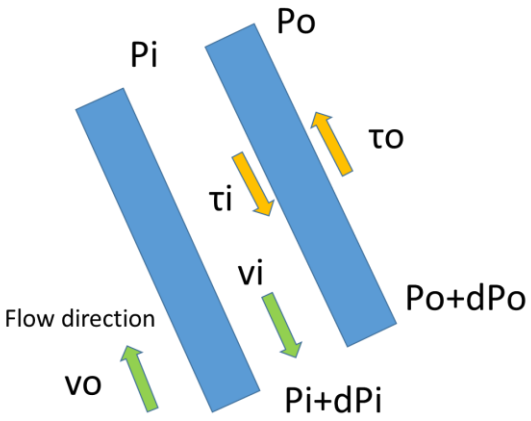

Figure 3 Schematic of fluid flow

The inner and annular pressures are calculated by

$$\frac{\partial P_i}{\partial s} = \rho_i g \cos\varphi - \frac{\lambda_i}{D_i}\frac{\rho_i v_i^2}{2} \quad (8)$$

$$\frac{\partial P_o}{\partial s} = \rho_o g \cos\varphi + \frac{\lambda_o}{D_w - D_o}\frac{\rho_o v_o^2}{2} \quad (9)$$

The shear forces on the inner and outer surfaces of tubular string due to fluid flow are calculated by

$$\tau_{wi} = \frac{\lambda_i}{4}\frac{\rho_i v_i^2}{2} \quad (10)$$

$$\tau_{wo} = \frac{\lambda_o}{4}\frac{\rho_o v_o^2}{2} \quad (11)$$

where λ_i and λ_o are the friction factors of inner and annular flows and are calculated by

$$\lambda_i = \begin{cases} \frac{64}{Re_i} & laminar\ flow(Re_i \le 2000) \\ \text{interpolation} & transient\ flow(2000 < Re_i \le 3000) \\ \frac{0.3164}{Re_i^{0.25}} & tubulent\ flow(Re_i > 3000) \end{cases} \quad (12)$$

$$\lambda_o = \begin{cases} \frac{96}{Re_o} & laminar\ flow(Re_o \le 2000) \\ \text{interpolation} & transient\ flow(2000 < Re_o \le 3000) \\ \frac{0.3164}{Re_o^{0.25}} & tubulent\ flow(Re_o > 3000) \end{cases} \quad (13)$$

where Re_i and Re_o are the Reynolds numbers for inner and annular flows.

Calculation Method

Finite difference scheme

For the convenience of derivation, Eq. 1 can be expressed as

$$\rho_s A_s \frac{\partial^2 u}{\partial t^2} = \frac{\partial}{\partial s}\left(EA_s\frac{\partial u}{\partial s}\right) + f + \mu N \quad (14)$$

where f is external load on tubular string per unit length except friction force and is calculated by $f = q_e \cos\varphi + \pi\tau_{wi}D_i - \pi\tau_{wo}D_o$.

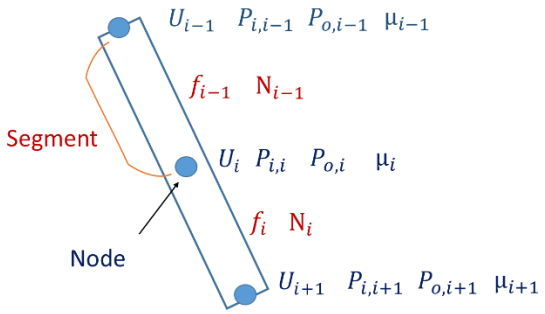

Figure 4 Schematic of discretized parameters on tubular string

Figure 4 shows the discretized parameters on tubular string. A segment of tubular string includes two nodes, in which axial displacement (U_i), pressures ($P_{i,i}$ and $P_{o,i}$), and friction factor (μ_i) are defined on nodes and external load (f_i) and contact force (N_i) are defined on segments. Therefore, the subscript "i" in U_i represents the left node of i-th segment or the right node of (i-1)-th segment, and the subscript "i" in f_i represents i-th segment.

To capture the changes between sliding friction force and sticking friction force, a rather small time interval must be adopted in the finite difference calculation. Then, an explicit finite difference scheme is more proper for calculation, because algorithm stability can be ensured under small time interval and less calculation time will be consumed by using the explicit scheme.

With the definitions of above discretized parameters, the explicit central difference scheme of Eq. 14 can be expressed as

$$(\rho_s A_s)_i \frac{{U_i}^{j+1}-2{U_i}^{j}+{U_i}^{j-1}}{\Delta t^2} = (EA_s)_i \frac{{U_{i+1}}^{j}-2{U_i}^{j}+{U_{i-1}}^{j}}{\Delta {s_i}^2} + \frac{{f_{i-1}}^{j}+{f_i}^{j}}{2} + {\mu_i}^{j} \frac{{N_{i-1}}^{j}+{N_i}^{j}}{2} \qquad 15$$

where, Δt is the time interval, the superscript "j" in ${U_i}^{j}$ represents the i-th time point.

Initial condition

In general, an equilibrium initial condition is given for calculation. In other words, the initial displacement satisfies Eq. 1 of which the right side is set to 0. The discretized scheme of initial displacement condition is expressed as

$$ {U_i}^{1} = u_{initial} \qquad 16$$

The discretized scheme of initial velocity condition is expressed as

$$ \frac{{U_i}^{2}-{U_i}^{0}}{2\Delta t} = v_{initial} \qquad 17$$

Note that the term ${U_i}^{0}$ in Eq. 17 can be eliminated by combing Eq. 17 and Eq. 15 while j=1.

Boundary condition

The top of the tubular string is tied to a hook, so that the axial displacement of the top of tubular string is equal to the vertical displacement of hook. Then, the top boundary condition is expressed as

$$ {U_1}^{j} = u_{hook} \qquad 18$$

In the tripping in or out operation, the axial force on bit is usually set to 0. In the drilling process, the axial force on bit is determined with bit-rock interaction model. For simplicity, the value of axial force on bit is given and then the bottom boundary condition is expressed as

$$ (EA_s)_n \frac{{U_{n+1}}^{j}-{U_{n-1}}^{j}}{2\Delta s_n} = F_{bit} \qquad 19$$

Note that the term ${U_{n+1}}^{j}$ in Eq. 19 can be eliminated by combing Eq. 19 and Eq. 15 while i=n.

Continuous condition

When two or more than two kinds of tubular strings are adopted, the relevant parameters such as tubular diameter, weight, etc., are different for different tubular strings. Then the continuous conditions on the node connecting to different tubular types should be satisfied. To be specific, the equivalent axial forces

on adjacent segments are continuous on this point. By combing the displacement equations on these two segments and continuous condition on this point, the finite difference scheme is expressed as

$$\left(\frac{(\rho_s A_s)_{i-1}\Delta s_{i-1}}{2}+\frac{(\rho_s A_s)_i \Delta s_i}{2}\right)\frac{U_i{}^{j+1}-2U_i{}^{j}+U_i{}^{j-1}}{\Delta t^2}=(EA_s)_{i-1}\frac{U_{i-1}{}^{j}}{\Delta s_{i-1}}-\left(\frac{(EA_s)_{i-1}}{\Delta s_{i-1}}+\frac{(EA_s)_i}{\Delta s_i}\right)U_i{}^{j}+(EA_s)_i\frac{U_{i+1}{}^{j}}{\Delta s_i}+\frac{\Delta s_{i-1}}{2}f_{i-1}{}^{j}+\frac{\Delta s_i}{2}f_i{}^{j}+\frac{\Delta s_{i-1}}{2}\mu_i^j N_{i-1}{}^{j}+\frac{\Delta s_i}{2}\mu_i^j N_i{}^{j}+(1-2\upsilon_{i-1})\left(P_{i,i}{}^{j}A_{i,i-1}-P_{o,i}{}^{j}A_{o,i-1}\right)-(1-2\upsilon_i)\left(P_{i,i}{}^{j}A_{i,i}-P_{o,i}{}^{j}A_{o,i}\right) \quad 20$$

Friction factor

As is discussed above, the value of friction factor can be calculated using Eq. 7.

For the sliding friction state, friction factor is determined by velocity direction, namely $\mu_i^{j+1}=-sign\left(V_i^{j+1}\right)\mu_d$, in which V_i^{j+1} is the axial velocity of i-th node at the end of (j+1)-th time interval.

For the sticking friction state, friction factor μ_i^{j+1} is determined from Eq. 15 while letting the left side equal to zero and setting the superscript j to j+1. If the absolute value of μ_i^{j+1} is larger than the maximum sticking friction factor μ_s, the value of μ_i^{j+1} is calculated with velocity direction, namely $\mu_i^{j+1}=-sign\left(V_i^{j+1}\right)\mu_d$.

Fluid flow

The finite difference schemes of Eqs. 8 and 9 are expressed as

$$\frac{P_{i,i+1}{}^{j+1}-P_{i,i}{}^{j+1}}{\Delta s_i}=\rho_{i,i}g\cos\varphi_i-\frac{\lambda_{i,i}}{D_{i,i}}\frac{\rho_i v_{i,i}^2}{2} \quad 21$$

$$\frac{P_{o,i+1}{}^{j+1}-P_{o,i}{}^{j+1}}{\Delta s_i}=\rho_{o,i}g\cos\varphi_i+\frac{\lambda_{o,i}}{D_{w,i}-D_{o,i}}\frac{\rho_o v_{o,i}^2}{2} \quad 22$$

If the pump rate is given, the inner and annular flow velocities in Eqs. 21 and 22 can be calculated. In general, if the annular back pressure namely $P_{o,1}{}^{j}$ is known, the distribution of annular pressure along wellbore can be obtained using Eq. 22. By letting the inner pressure equal to annular pressure at the drill bit, the distribution of inner pressure along wellbore can be obtained using Eq. 21.

Results and discussions

On the basis of the above model and calculation method, the mechanical behaviors of tubular strings under tripping in, tripping out, and sliding drilling operations are studied. A horizontal well is drilled of which the depth of kick off point is 1000m, curvature radius of building section is 300m, inclination angle of the horizontal section is π/2, and well depth is 2700m. A 5-inch drill pipe is adopted of which tubular string weight in air per unit length is 29.05kg/m. Bingham drill fluid is used of which the density is 1.1g/cm^3, plastic viscosity is 20 mPa.s, and dynamic shear stress is 3Pa.

In the numerical simulation, to reveal the transition between sticking friction and sliding friction, the time interval should be very small. The time interval is set to 2e-4s, segment length is set to 9m, and operation time is set to 1 min. It takes about 1 min to obtain the results.

Tripping out

In the tripping out operation, axial force on bit is set to 0 and the top axial displacement is controlled by hook. Two kinds of hook control modes, including trapezoidal and parabolic modes, are adopted and given in Figure 5.

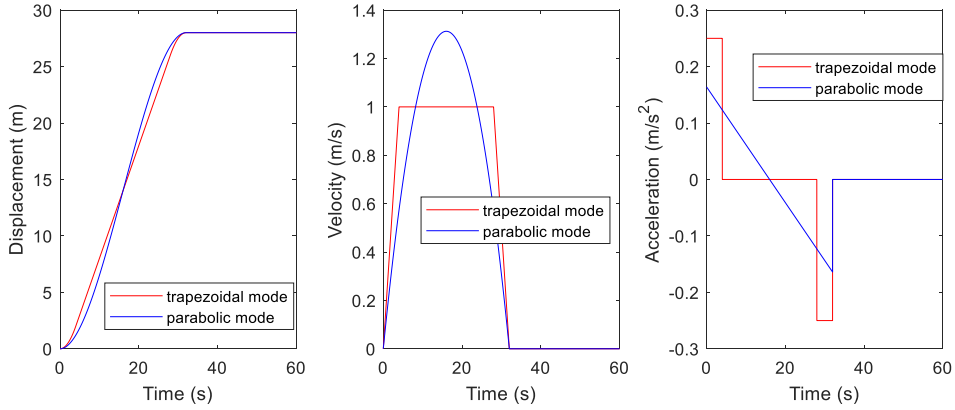

Figure 5 Displacements, velocities, and accelerations for different hook control modes

Figure 6 shows the results for trapezoidal mode based on Miska's (2015) model. In Miska's model, the entire tubular string is assumed to move synchronously, and stress vibration propagation along tubular string is neglected; so, the hook load changes synchronously with acceleration. However, complex mechanical behaviors of tubular string may not be revealed with the introduction of the assumption in Miska's model. To overcome this shortcoming, the above assumption is taken out in the new model.

Generally, friction force is in opposite direction to the tripping direction, and then the friction factor can be set to a constant. Figure 6 shows the results for trapezoidal mode based on the new model of constant friction factor. The results show that the maximum hook load for the new model is larger than Miska's model. Therefore, neglecting stress wave propagation will lead to underestimation of axial force.

Tubular movement still exists after tripping out operation for the constant friction factor model. This is because the direction change of friction force is not included. To overcome this shortcoming, velocity-dependent friction model is adopted in this paper. Figure 7 shows the results based on the new model. The results show that the magnitude of displacement decreases rather fast and then vanishes due to the effect of friction force. Therefore, the new model is superior to the previous two models.

The stable hook load after tripping out operation is smaller than the initial hook load because of the nonlinearity of friction force. Figure 8 shows friction states along the tubular string at the end of tripping out operation. The results show that some segments of tubular string are in sliding friction state and the others are in sticking friction state. Considering that the sticking friction force is usually smaller than the sliding friction force, the hook load at the end of tripping out operation is usually smaller than that at the start.

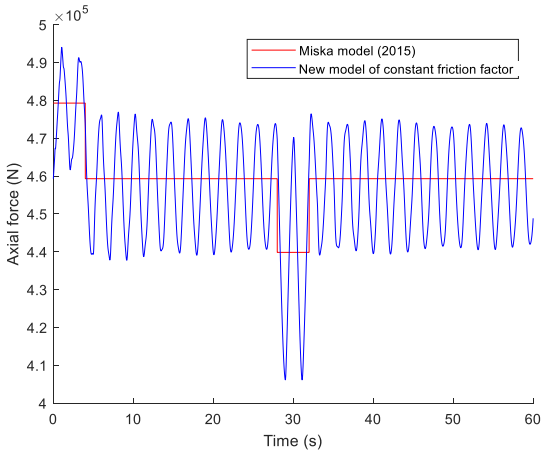

Figure 6 Axial forces on hook for tripping out operation for two previous models (no fluid)

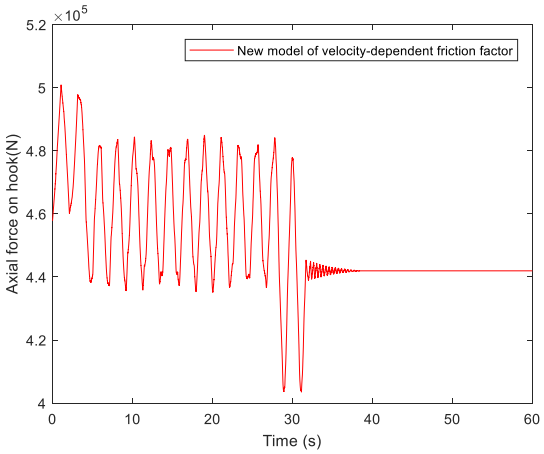

Figure 7 Axial forces on hook for tripping out operation for the new model (no fluid)

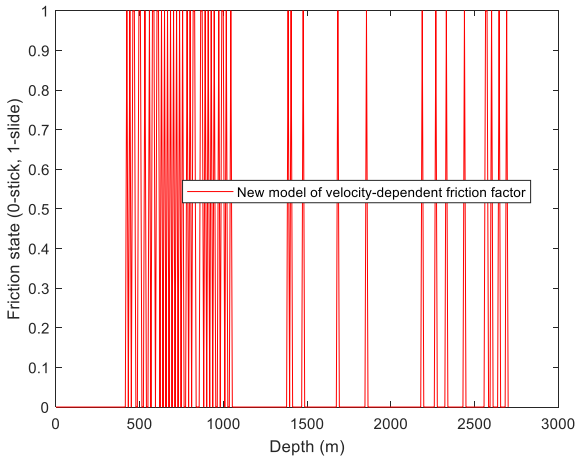

Figure 8 Friction states at the end of tripping out operation (no fluid)

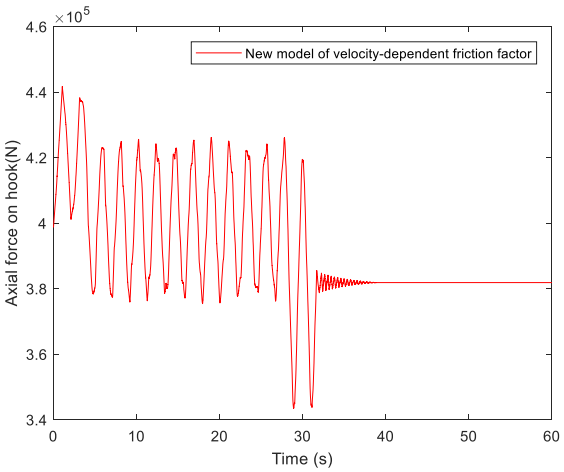

Figure 9 Axial forces on hook for tripping out operation for the new model (trapezoidal mode)

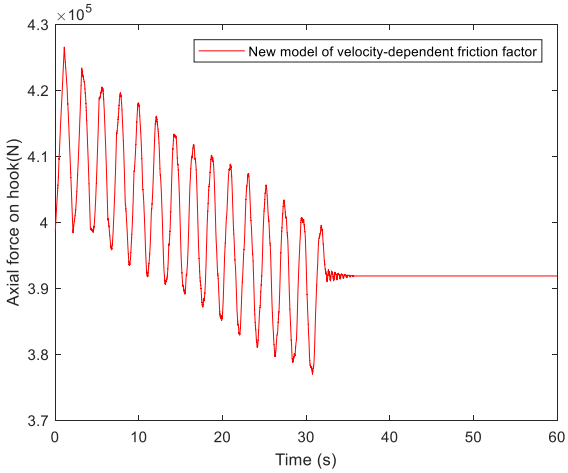

Figure 10 Axial forces on hook for tripping out operation for the new model (parabolic mode)

Figure 9 shows the results for trapezoidal mode based on the new model while further considering drill fluid. The hook load is decreased due to the existence of buoyancy force. There is almost no change in the magnitude of displacement with and without drill fluid. Therefore, drill fluid has negligible effect on displacement magnitude in tripping operation.

Figure 10 shows the results for parabolic mode based on the new model. By comparing results in Figure 9 and Figure 10, we can see that the maximum hook load due to vibration under parabolic mode is smaller than that under trapezoidal mode. Meanwhile, the magnitude of hook load vibration also becomes smaller under parabolic mode.

Tripping in

Figure 11, Figure 12, Figure 13, and Figure 14 show the relevant results in tripping in operations that similar conclusions can be obtained. For example, the stable hook load after tripping in operation is larger than the initial hook load because of the nonlinearity of friction force.
Figure 9 and Figure 13 show that oscillation magnitudes at the deceleration stage in tripping out operation and at the acceleration stage in tripping in operation are much larger than that under other stages for trapezoidal mode. However, oscillation magnitude is rather uniform in tripping in and out operations for parabolic mode and smaller than that for trapezoidal mode. Therefore, trapezoidal mode is superior to parabolic mode for tripping operations. Considering that velocities and acceleration change more gently

in parabolic mode than that in trapezoidal mode shown in Figure 5. Gentler hook control mode can decrease vibration magnitude, and thus increase operation safety factor.

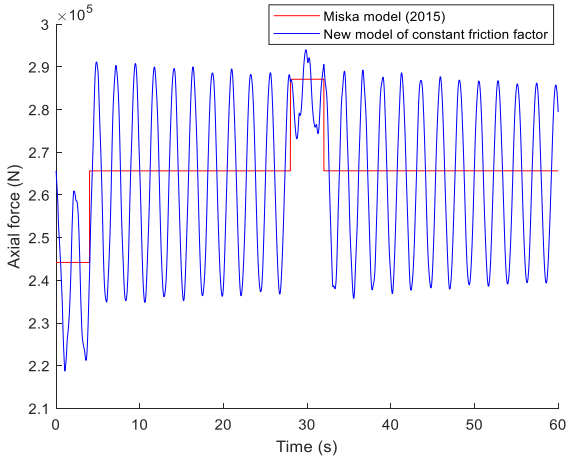

Figure 11 Axial forces on hook for tripping in operation for two previous models (no fluid)

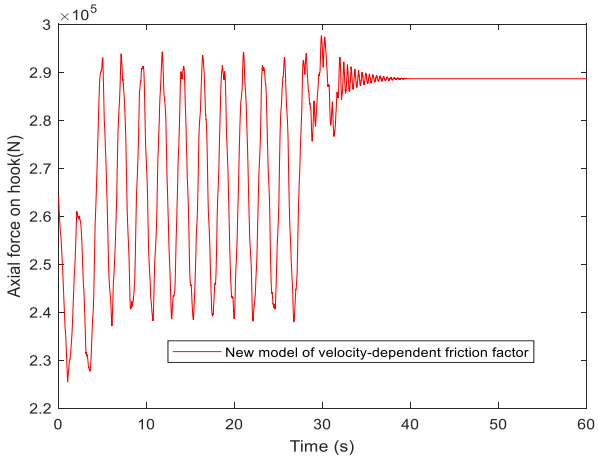

Figure 12 Axial forces on hook for tripping in operation for the new model (no fluid)

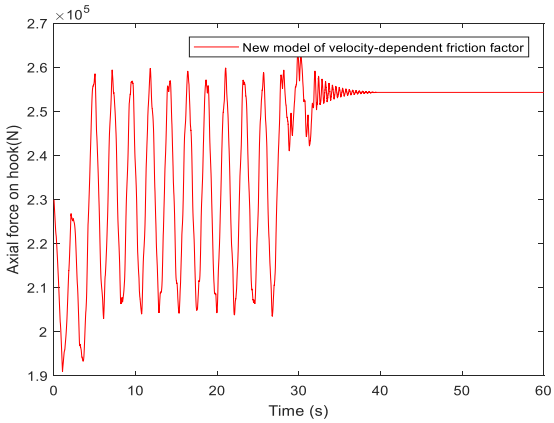

Figure 13 Axial forces on hook for tripping in operation for the new model (trapezoidal mode)

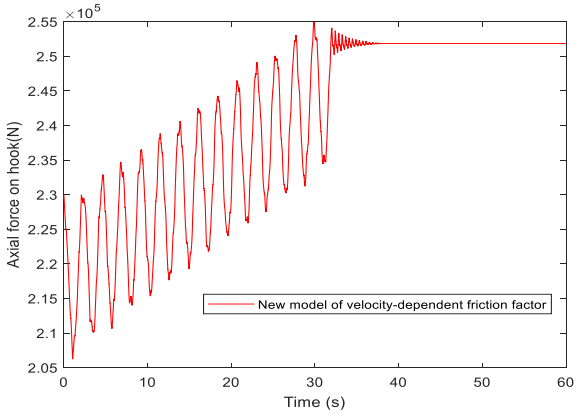

Figure 14 Axial forces on hook for tripping in operation for the new model (parabolic mode)

Sliding drilling

In the sliding drilling operation, axial force on bit is set to the negative value of WOB. The top displacement condition is equal to the integral of rate of penetration (ROP) and time.

Figure 15 shows the hook load when WOB=100kN and ROP=36m/h. After a short transition stage, hook load becomes stable and is approximately equal to 212kN. Figure 16 shows the hook load when WOB=50kN and ROP=36m/h, and the stable force on hook is approximately equal to 280kN, which is about 68kN larger than that for WOB=100kN. Therefore, with the decrease of WOB, hook load increases, and the increasing magnitude of hook load is larger than the decreasing magnitude of WOB.

In actual sliding drilling process, WOB is not a constant value but changes with time. WOB is divided into two parts: average WOB and fluctuant WOB. Figure 17 shows the hook load when WOB=100kN+50kN*sin(2πt). After a short transition stage, hook load vibrates with the magnitude of 10kN in the stable oscillation stage. Thus, stress oscillation is weakened in the upward propagation along the tubular string from drill bit to hook.

Although the average WOB in Figure 17 is equal to WOB in Figure 15, the stable hook load (about 306kN) for vibrating WOB is larger than that for constant WOB. Therefore, vibrating WOB can decrease drag on the entire string.

By comparing results in Figure 17 and Figure 18, we can see that the value of stable hook load is nearly irrelevant to the frequency of WOB oscillation. However, changes in the oscillation magnitude of WOB result in changes in the stable hook load as shown in Figure 19 (about 244kN). With the increase in oscillation magnitudes of WOB from 0, 25kN, to 50kN, the hook loads increase from 212kN, 244kN, to 306kN. The increasing range of hook load also becomes larger with the increase in oscillation magnitudes of WOB.

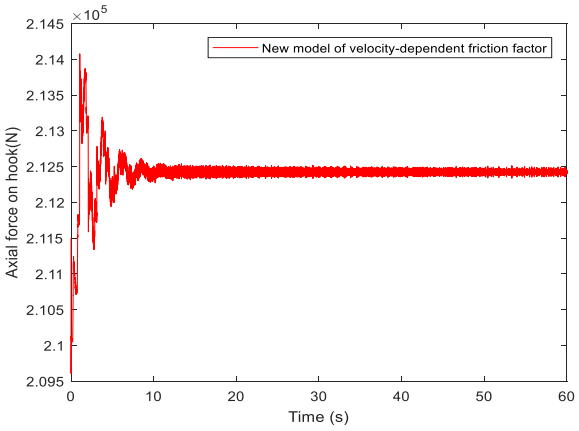

Figure 15 Axial forces on hook for sliding drilling operation (WOB=100kN)

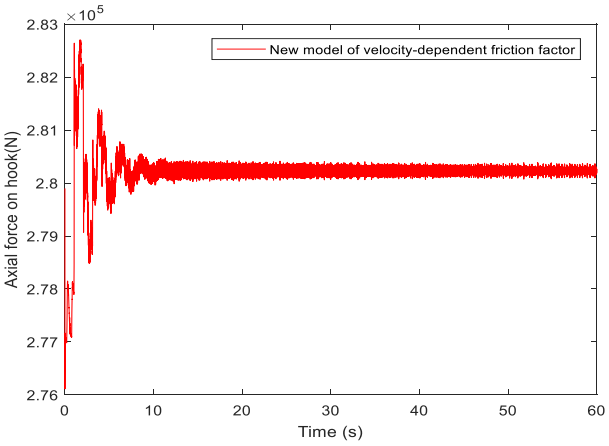

Figure 16 Axial forces on hook for sliding drilling operation (WOB=50kN)

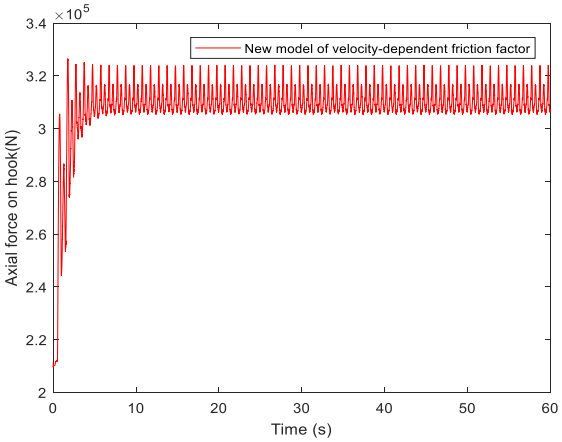

*Figure 17 Axial forces on hook for sliding drilling operation (WOB=100kN+50kN*sin(2πt))*

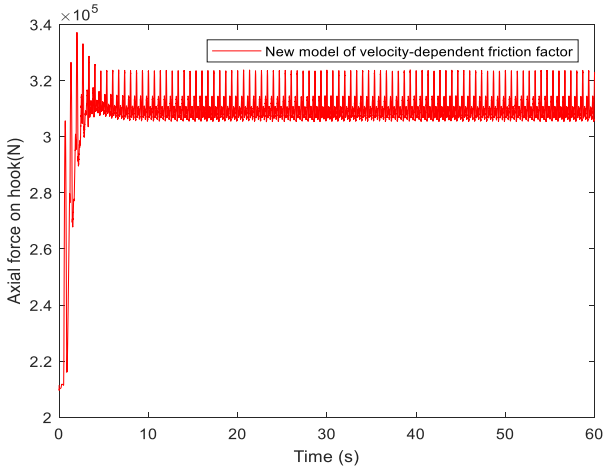

*Figure 18 Axial forces on hook for sliding drilling operation (WOB=100kN+50kN*sin(3πt))*

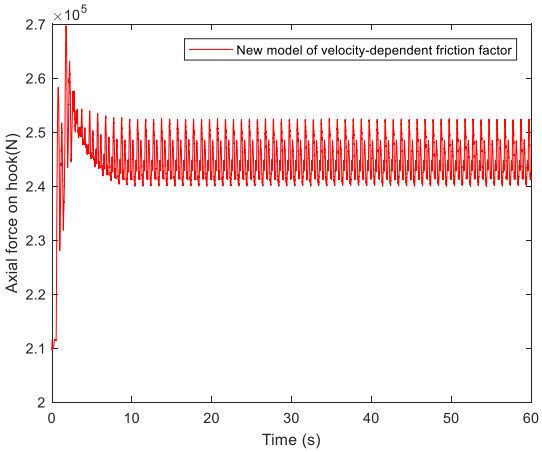

*Figure 19 Axial forces on hook for sliding drilling operation (WOB=100kN+25kN*sin(2πt))*

Conclusions

From the above analyses, we obtain the following conclusions:

(1) In the new model, the effects of tubular displacement, drill fluid, and velocity-dependent friction force are all taken into consideration, which overcomes the shortcomings in the previous model. The new model can be used for calculating the dynamic mechanical behaviors of tubular string under tripping in, tripping out, and sliding drilling operations.

(2) Explicit central finite difference scheme of tubular displacement equation and Karnopp's friction model are adopted in the calculation. Results indicate that the calculation algorithm is fast and stable.

(3) Neglecting tubular displacement leads to underestimation of maximum hook load in tripping out operation and overestimation of minimum hook load in tripping in operation, which further leads to risky design results.

(4) Friction force can substantially inhibit tubular movement. For example, the magnitude of displacement decreases rather fast and then vanishes after tripping in and out operations due to friction force.

(5) The nonlinearity of friction force in tubular displacement cannot be neglected. For example, the stable hook loads after tripping in and out operations are usually different from the initial values.

(6) Oscillation magnitude under trapezoidal mode is smaller than that under parabolic mode for tripping operations. Therefore, a gentler hook control mode can ensure larger operation safety factor.

(7) Applying external vibrating force on tubular string can decrease the drag. For example, vibrating WOB can increase hook load compared with constant WOB. The effect of drag reduction due to displacement force increases with the increase in oscillation magnitude.

References

Johancsik, C. A., Friesen, D. B., & Dawson, R. 1984. Torque and Drag in Directional Wells-Prediction and Measurement. Society of Petroleum Engineers. doi:10.2118/11380-PA.

Ho, H-S. 1988. An Improved Modeling Program for Computing the Torque and Drag in Directional and Deep Wells. Society of Petroleum Engineers. doi:10.2118/18047-MS.

Gao, D. 1994. Prediction and control of wellbore trajectory. Dongying: China University of Petroleum Press.

Wu, J. and Juvkam-Wold, HC. 1995. The Effect of Wellbore Curvature on Tubular Buckling and Lockup. Journal of Energy Resources Technology, 117 (3): 214-218. SPE-139824-PA.

McSpadden A, Newman K. 2002. Development of a Stiff-String Forces Model for Coiled Tubing. SPE/ICoTA Coiled Tubing Conference and Exhibition, Houston, Texas.

Mitchell, R. F., & Samuel, R. (2009, March 1). How Good Is the Torque/Drag Model? Society of Petroleum Engineers. doi:10.2118/105068-PA

Mitchell R F, Bjorset A, Grindhaug G. 2015. Drillstring Analysis With a Discrete Torque/Drag Model. SPE Drilling & Completion, 30(01): 5-16.

Zhang, Y., & Samuel, R. (2019, September 23). Engineers' Dilemma: When to Use Soft String and Stiff String Torque and Drag Models. Society of Petroleum Engineers. doi:10.2118/196205-MS

Miska, S. Z., Zamanipour, Z., Merlo, A., & Porche, M. N. 2015. Dynamic Soft String Model and Its Practical Application. Society of Petroleum Engineers. doi:10.2118/173084-MS.

Robello Samuel, Friction factors: What are they for torque, drag, vibration, bottom hole assembly and transient surge/swab analyses? Journal of Petroleum Science and Engineering, Volume 73, Issues 3–4, September 2010, Pages 258-266. doi.org/10.1016/j.petrol.2010.07.007

Karnopp D. Computer Simulation of Stick-Slip Friction in Mechanical Dynamic Systems. 1985. ASME. J. Dyn. Sys., Meas., Control., 107(1):100-103. doi:10.1115/1.3140698.